Uptake of Materials by the Intact Liver

THE EXCHANGE OF GLUCOSE ACROSS THE CELL MEMBRANES

CARL A. GORESKY and BRITA E. NADEAU

From the McGill University Medical Clinic in the Montreal General Hospital, Montreal, Quebec, Canada

ABSTRACT D-Glucose equilibrates within liver cells. We have studied its process of entry into and exit from these cells with the multiple indicator dilution technique. Labeled red cells (a vascular indicator), labeled sucrose (an extracellular reference), and labeled D-glucose were rapidly injected into the portal vein, and from serially sampled hepatic venous blood, normalized outflow-time patterns were obtained. The labeled red cell curve rises to an early high peak, and decays rapidly; and that for sucrose reaches a later and lower peak and decays less rapidly, but generates an equivalent area. The curve for labeled D-glucose begins with that for labeled sucrose, gradually rises to a peak which is later and substantially lower than that for sucrose, and then decreases slowly. At high glucose levels this curve assumes a squared-off shape, rises fairly quickly to its highest level, at the time of the sucrose peak, and then slowly decreases. Phlorizin and galactose infusion result in the emergence of a pronounced early peak, under the sucrose peak; and the curve for tracer L-glucose approaches that for sucrose.

We resolve from the D-glucose curves, by model analysis, two components: throughout material, which has not entered the cells; and exchanging material, which has entered and later returned to the circulation. The analysis provides estimates of the kinetic entrance and exit coefficients; and from these, saturation of both the entrance and exit processes was evident. The characteristic transport parameters were determined. For both entrance and exit, a common K_m, 2,170 mg/100 ml, and transport maximum, 5.13 mg s^{-1} (ml intracellular fluid)$^{-1}$, were found. Both these values are exceedingly large. Several other phenomena were defined which additionally characterize the transport process: phlorizin and galactose produced competitive inhibition; the transport process was found to be relatively stereospecific; and sudden infusion of hypertonic glucose produced counter-transport of labeled D-glucose.

INTRODUCTION

The liver serves as one of the primary organs in glucose homeostasis. Under ordinary circumstances, in the intact animal, it serves to remove glucose from the portal venous blood after eating and to add glucose to the circulation during fasting (1). The set point for this change-over is regulated by insulin (2, 3). Some years ago Cahill, Ashmore, Earle, and Zottu investigated the intracellular concentration of free glucose in the liver and found it to be equivalent to the concomitant plasma concentration, whether or not the net activity of the liver was one of glucose uptake or glucose output (4). They also demonstrated that, under both conditions, tracer D-glucose injected intravenously reached equivalent activities in liver and plasma water within 5 min. Within the limitations of their data, these authors felt that the entry of D-glucose into the liver cell was relatively free, and that it probably proceeded by passive diffusion.

It is our purpose here to explore this entry process in more detail, to produce evidence that it is carrier mediated, and to quantitate the parameters which characterize it. In 1967, we examined tracer D-glucose entry into the intact liver, by means of the multiple indicator dilution technique, and reported qualitatively that raising the plasma glucose levels slowed the relative rate of entry of tracer D-glucose and that the rate of entry of tracer L-glucose was very slow (5). Simultaneously,

The experimental findings but not their analysis were presented in preliminary form at the Annual Meeting of the American Society for Clinical Investigation in Atlantic City, N. J., May 1967.

Received for publication 12 February 1973 and in revised form 1 October 1973.

Williams, Exton, Park, and Regen explored the entry process, utilizing the isolated perfused liver (6). They showed, by tissue sampling, that although equilibration within the liver cells of D-glucose (tracer and load) occurs within 10 min, the process is incomplete in 2 min, and tracer L-glucose enters liver cells, but equilibrates only over a period of approximately 40 min. These authors also used a lumped model analysis to obtain preliminary estimates of kinetic parameters from outflow curves resulting from the steady infusion of tracer D-glucose and an extracellular reference material, inulin. Here we complement, extend, and complete these previous studies. We use the multiple indicator dilution technique to obtain data from the intact liver over a wide range of glucose concentrations. We utilize our recently developed kinetic modeling, which takes into account the distribution of the uptake process in space as well as time (7, 8), to provide precise estimates of both the kinetic parameters from dilution curves and the characteristic parameters of the transport process, the Michaelis-type constant (K_m), and the maximal rate of transport (V_{max}).

METHODS

We use the rapid single injection multiple indicator dilution technique (7) as our experimental approach and inject simultaneously into the portal vein ^{51}Cr-labeled red cells (a vascular reference), ^{14}C-labeled sucrose (a reference extracellular material, which distributes into the extracellular space in a flow-limited fashion and does not enter liver cells during a single passage [4, 8]), and ^{3}H-labeled D-glucose. The experiments are carried out in anesthetized dogs, in which glucose infusions and insulin administration have been used to manipulate the endogenous glucose levels. The injection mixture was constituted by adding the ^{14}C and ^{3}H tracers to plasma obtained from the animal just before the run; and then by adding labeled red cells, in amounts adequate to match the hematocrit to that of the blood in the animal. The latter were added to the injection mixture only at the time of the run to avoid red cell carriage of the tracer glucose (isotopic equilibration of this tracer in these red cells ordinarily requires about 4 h [5]). Several additional studies were carried out to characterize the process involved in the handling of the labeled glucose: phlorizin and galactose were infused, to demonstrate competitive phenomena; L-galactose transport was studied, to document the effect of stereospecificity; the transport of β-methyl D-glucoside was examined, to demonstrate the effect of a change in molecular architecture; and countertransport of label was induced.

Special materials. The following special materials were used: $Na_2{}^{51}CrO_7$ solution, 5–10,000 Ci/mM (Charles E. Frosst and Co., Montreal, Quebec, Canada); D-[U-^{14}C]-sucrose 3–5 mCi/mM; D-[1-^{3}H]glucose, 0.2–1.6 Ci/mM; or D-[2-^{3}H]glucose, 0.6 Ci/mM (New England Nuclear, Boston, Mass.); L-[1-^{3}H]glucose, 1.6 Ci/mM; and β-methyl D-[^{3}H]glucoside, 0.2 Ci/mM (International Chemical and Nuclear Corp., City of Industry, Calif.).

RESULTS

The outflow patterns of two typical D-glucose experiments are illustrated in Fig. 1. In each, the labeled sucrose curve is displaced from the labeled red cell curve in the manner expected, as a result of its extravascular flow-limited distribution out to the cell surface (8): the sucrose outflow fractional recoveries per milliliter are lower on the upslope, the sucrose peak is lower, and the downslope decays more slowly. The curves for both these reference substances are corrected for recirculation by linear extrapolation on the semilogarithmic plot, in the usual manner. At the normal plasma glucose level, the labeled glucose curve rises gradually to a peak which is later and substantially lower than the sucrose

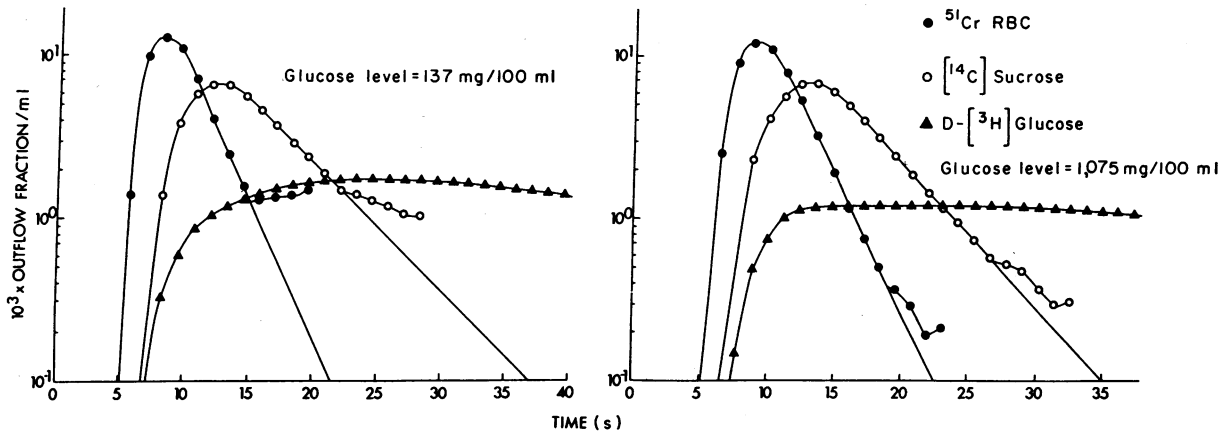

FIGURE 1 Change in the outflow profile of labeled glucose with change in the plasma glucose levels. Abscissas: time in seconds. Ordinates: outflow fractional recovery per milliliter (fraction of the total injected activity per milliliter), plotted on a logarithmic scale. The values are plotted at mid-intervals. The two experiments illustrated are numbered 3 and 9 in the Tables. The time delay in the collecting system was 2.21 s, in each of these experiments.

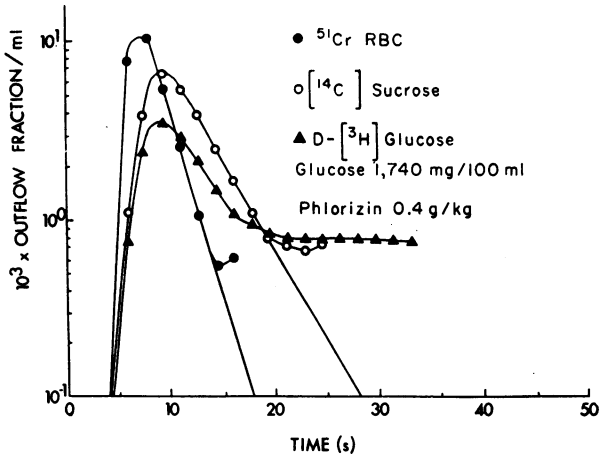

FIGURE 2 Outflow pattern during intraportal phlorizin infusion, at a high glucose level. This experiment was numbered 18 in the Tables.

peak, and then slowly begins to drop. At the high glucose level, the labeled glucose curve has a squared-off shape. It rises fairly quickly to its highest level, at the time of the labeled sucrose peak, and thereafter changes little for a prolonged period. There is no simple extrapolation procedure which would lead to recovery of the primary labeled glucose curve in either case.

Fig. 2 illustrates the dramatic effect of a continuing intraportal infusion of phlorizin on the shape of the labeled D-glucose curve. An early peak has emerged from the tracer D-glucose curve, which is related to and contained within the reference sucrose curve. On the downslope this curve approaches and crosses over the sucrose curve and becomes higher than the recirculating portion of that curve. It is therefore reasonable to assume that the primary curve for this label must be made up

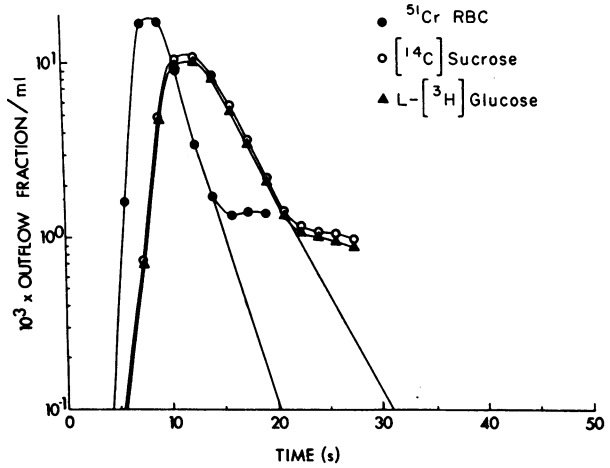

FIGURE 3 A labeled L-glucose experiment. This experiment was numbered 25 in the Tables.

of two components, an early peak and a later tailing. In the presence of a galactose load, the tracer D-glucose curve (not illustrated here) has a form intermediate between that of the phlorizin experiment and that found in the presence of a high glucose level.

The further evolution of this series of changes is depicted in Fig. 3, the illustration of an experiment in which labeled L-glucose was used. The labeled L-glucose curve is slightly lower than and almost parallel to the labeled sucrose curve. The labeled L-glucose curve thus consists almost entirely of a first major peak. Since this sugar is not metabolized (9), we can hypothesize that there is here again a second component to the primary curve, a low and prolonged tailing, representing the return of the sugar to the circulation, and indistinguish-

TABLE I
Transit Time and Flow Data from Dilution Curves

Exp. no.	Body wt	Liver wt	Hepatic perfusion	$\bar{t}_{RBC}$*	$\bar{t}_{sucrose}$*	Sucrose‡ extravascular space
	kg	*g*	*ml s^{-1} g^{-1}*	*s*	*s*	*(ml plasma) g^{-1}*
D-Glucose experiments						
1	16.0	482	0.022	7.71	14.04	0.089
2	12.5	246	0.028	5.05	10.87	0.090
3	14.0	251	0.059	6.77	12.76	0.183
4	14.0	309	0.031	8.13	14.93	0.116
5	18.0	395	0.024	9.47	18.11	0.116
6	14.0	539	0.031	5.25	12.25	0.135
7	14.0	298	0.047	5.27	9.51	0.124
8	9.0	267	0.042	7.73	11.53	0.096
9	21.0	577	0.025	7.79	12.98	0.087
10	15.0	505	0.033	8.41	14.95	0.168
11	20.0	493	0.015	12.82	21.94	0.097
12	18.0	460	0.023	9.16	14.78	0.087
13	16.0	576	0.040	6.95	14.23	0.160
14	16.0	449	0.017	12.44	24.96	0.109
15	17.5	401	0.028	5.61	10.75	0.078
16	19.0	424	0.020	12.56	22.27	0.103
Phlorizin infusion						
17	20.0	573	0.035	8.61	12.63	0.090
18	14.0	568	0.036	5.44	9.28	0.118
19	15.5	743	0.020	9.85	17.98	0.130
D-Galactose loading						
20	18.0	570	0.039	5.51	8.56	0.074
21	16.0	488	0.052	3.52	6.04	0.102
L-Glucose experiments						
22	9.0	172	0.055	11.51	17.86	0.206
23	14.0	318	0.036	6.51	10.98	0.103
24	10.0	235	0.028	7.22	14.50	0.120
25	20.0	429	0.026	8.10	13.22	0.068
β-Methyl D-glucoside experiments						
26	12.0	351	0.049	7.23	11.06	0.146
27	15.0	526	0.027	7.63	11.36	0.072
28	20.0	785	0.028	8.43	16.64	0.154
29	16.0	499	0.019	8.74	15.03	0.062

* The mean transit times were corrected for the catheter transit times.
‡ The sucrose extravascular space was calculated as the product of the plasma flow and the difference between the labeled sucrose and red cell mean transit times.

able from recirculation. The curve for labeled β-methyl D-glucoside is similar to that for labeled L-glucose in Fig. 3, but approaches the reference labeled sucrose curve even more closely.

In Table I we have listed the parameters which can be obtained directly from the curves. These include values for hepatic perfusion (i.e., for flow per unit weight of tissue), and for the mean transit times for labeled red cells and labeled sucrose. The outflow recoveries for labeled red cells and labeled sucrose are equivalent (the ratio of the area under the labeled sucrose curve to that under the labeled red cell curve was 1.023±0.053 [SD]).

The transport rate constants. To provide a basis for the interpretation of these experiments, we initially utilized for their analysis a kinetic model which we developed for a set of galactose experiments (8). The fundamental considerations used in the development of this modeling (see Fig. 4) are the following:

(*a*) *A conservation equation.* Longitudinal transport of label along the sinusoid is assumed to occur only by the bulk transport mechanism of flow, within the times being considered. At each point along the length, net change in the total accessible label in the system is assumed to occur only by two processes: flow, or intracellular sequestration, which effectively removes it from the system.

(*b*) *Essential continuity between the vascular and extracellular spaces of the liver.* The extracellular space, the space of Disse, is separated from the cellular space only by a thin lining perforated by relatively large holes, and the glucose label will undergo flow-limited distribution into this space. We will assume that, for the small molecular weight species, the ground substance in the extracellular space imposes no steric restrictions on distribution.

(*c*) *A transport equation.* Basically, this is the classical equation which has been used for well-stirred two-compartment isolated cell systems. It is presented here in a form which provides for the spatial arrangements of the hepatic cells. The rate of change of material in the hepatic cells is set equal to the difference between membrane carrier entrance and exit fluxes, less any rate of absolute removal or sequestration of glucose label from the free intracellular pool. These assumptions result in the following equation:

$$\frac{\partial z(x,t)}{\partial t} = \frac{P_1'S}{C}\,u(x,t) - \frac{P_2'S}{C}\,z(x,t) - k_3 z(x,t),$$

where $z(x, t)$ = the concentration in the hepatic cells at a distance x from the origin or input of the sinusoid, at a time t; $u(x, t)$ = the corresponding concentration both in the sinusoid and at the surface of the liver cells; S/C = the ratio between the active transport surface

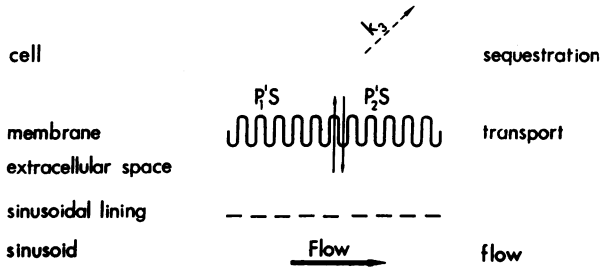

FIGURE 4 A diagrammatic representation of the modeling. In this illustration γ would be the ratio between the extracellular space and the sinusoidal plasma space; and θ, the ratio between the cellular space and the sinusoidal plasma space.

of the cells fronting a sinusoid (a highly mammillated surface, in the case of the liver cells) and their volume; P_1', P_2' = the membrane carrier transport coefficients, which are analogues of and have the same units ($cm \cdot s^{-1}$) as permeability coefficients, and k_3 = a sequestration rate constant. For the purposes of convenience we then set $k_1 = P_1'S/C$, and $k_2 = P_2'S/C$, and note that when the transport process is equilibrative, $P_1' = P_2'$ and $k_1 = k_2$.

The picture which results from the single sinusoid modeling is one in which there is flow-limited distribution of the glucose label out to the hepatic cell membrane, passage of the label across that membrane, and subsequent intracellular sequestration. It is clear that the net effect of the processes will, to a major extent, be governed by the flow in each sinusoid. This was assumed to vary and, from previous evidence (10), it was assumed that the large vessel transit times were common. When we examined the solution to this complete modeling, we found that we could derive, from the relationship between the tracer glucose and two reference curves, numerical estimates of the following parameters of the hepatic system: γ = the extracellular space ratio, the ratio between the extracellular space and the sinusoidal plasma space; t_o = the large vessel transit time; k_2 = the cellular efflux rate constant (the lumped parameter $P_2'S/C$); $k_1\theta/(1+\gamma)$ = the product of the cellular influx rate constant k_1 (the lumped parameter $P_1'S/C$) and the ratio $\theta/(1+\gamma)$, the ratio of the cellular space to the total accessible space, sinusoidal plus extracellular, outside the cells; and k_3 = the sequestration rate constant.

When the glucose curves were analyzed by means of this modeling we found that the fitted sequestration constant was an exceedingly small positive or negative number, and it appeared that no appreciable proportion of the labeled D-glucose was being sequestered by intracellular metabolic processes. This is not very surprising, if we consider that, in their experiments, Williams et al. (6) were unable to demonstrate measurable amounts of labeled phosphorylated intermediates by mixed bed resin

extraction of deproteinized extracts of liver, obtained 2 min after beginning a steady infusion of labeled D-glucose.

We therefore continued our analysis of these experiments, setting the sequestration constant of the modeling equal to zero. Optimized values for the four parameters γ, t_o, k_2, and $k_1\theta/(1+\gamma)$ were determined. Those for γ and t_o were determined from the relation between the sucrose and vascular reference curves (8); and the transport parameters $k_1\theta/(1+\gamma)$ and k_2 were

TABLE II

Glucose and Galactose Concentrations; and Derived Parameters

Exp. no.	Plasma glucose concentration	Plasma galactose concentration	Hct	Original curves			Corrected curves*		
				γ	$\frac{k_1\theta}{1+\gamma}$	k_2	γ	$\frac{k_1\theta}{1+\gamma}$	k_2
	mg/100 ml	*mg/100 ml*			s^{-1}	s^{-1}		s^{-1}	s^{-1}
D-Glucose experiments									
1	87		0.36	1.008	0.658	0.370	1.116	0.705	0.370
2	103		0.45	1.834	0.532	0.196	1.977	0.592	0.199
3	138		0.48	1.127	0.412	0.225	1.008	0.376	0.226
4‡	170		0.45	1.230	0.398	0.168	1.415	0.459	0.183
5‡§	392		0.44	0.988	0.172	0.087	1.157	0.194	0.091
6‡	414		0.38	1.957	0.371	0.178	2.209	0.613	0.237
7‡	713		0.38	0.547	0.300	0.193	0.719	0.421	0.206
8‡	765		0.40	0.921	0.374	0.197	1.124	0.430	0.200
9‡	1,075		0.33	0.855	0.311	0.129	0.923	0.333	0.135
10‡	1,436		0.22	1.114	0.323	0.182	1.003	0.308	0.182
11‡	1,458		0.29	0.908	0.390	0.142	0.981	0.413	0.144
12‡	1,752		0.33	0.627	0.207	0.097	0.898	0.280	0.107
13‖	90		0.45	1.673	0.450	0.141	1.810	0.787	0.259
14‖	56		0.49	1.383	0.409	0.159	1.468	0.431	0.165
15‖	53		0.46	0.964	0.296	0.209	1.077	0.434	0.232
16‖	44		0.47	1.085	0.428	0.216	1.210	0.461	0.219
Phlorizin infusion									
17¶	771		0.36	0.413	0.047	0.021	0.435	0.049	0.021
18¶	1,741		0.15	0.845	0.109	0.060	1.225	0.136	0.049
19¶	1,852		0.20	0.858	0.054	0.019	0.859	0.057	0.020
D-Galactose loading									
20**	124	402	0.38	0.643	0.240	0.141	—	—	—
21**	133	415	0.22	0.690	0.273	0.219	—	—	—
L-Glucose experiments									
22	124		0.41	0.548	0.004	0.002	0.564	0.004	0.004
23	125		0.36	0.897	0.012	0.004	0.972	0.013	0.004
24	131		0.41	1.296	0.012	0.003	1.356	0.013	0.003
25	135		0.49	0.762	0.004	0.002	0.847	0.004	0.004
β-Methyl D-glucoside experiments									
26	96		0.22	0.658	0.023	0.016	0.731	0.004	0.025
27	97		0.29	0.442	0.002	0.006	0.552	0.002	0.006
28	102		0.33	1.481	0.011	0.016	1.499	0.010	0.001
29	108		0.48	0.743	0.006	0.014	0.972	0.007	0.014

* These curves were corrected for catheter delay and distortion.

‡ D-Glucose was infused for 40 min before and during the run.

§ This animal was probably suffering from early distemper.

‖ Insulin was given.

¶ Phlorizin (0.24 g/kg) was infused into the portal vein before and during the run. Systemic hypotension was avoided.

** D-Galactose was infused for 40 min before and during the run.

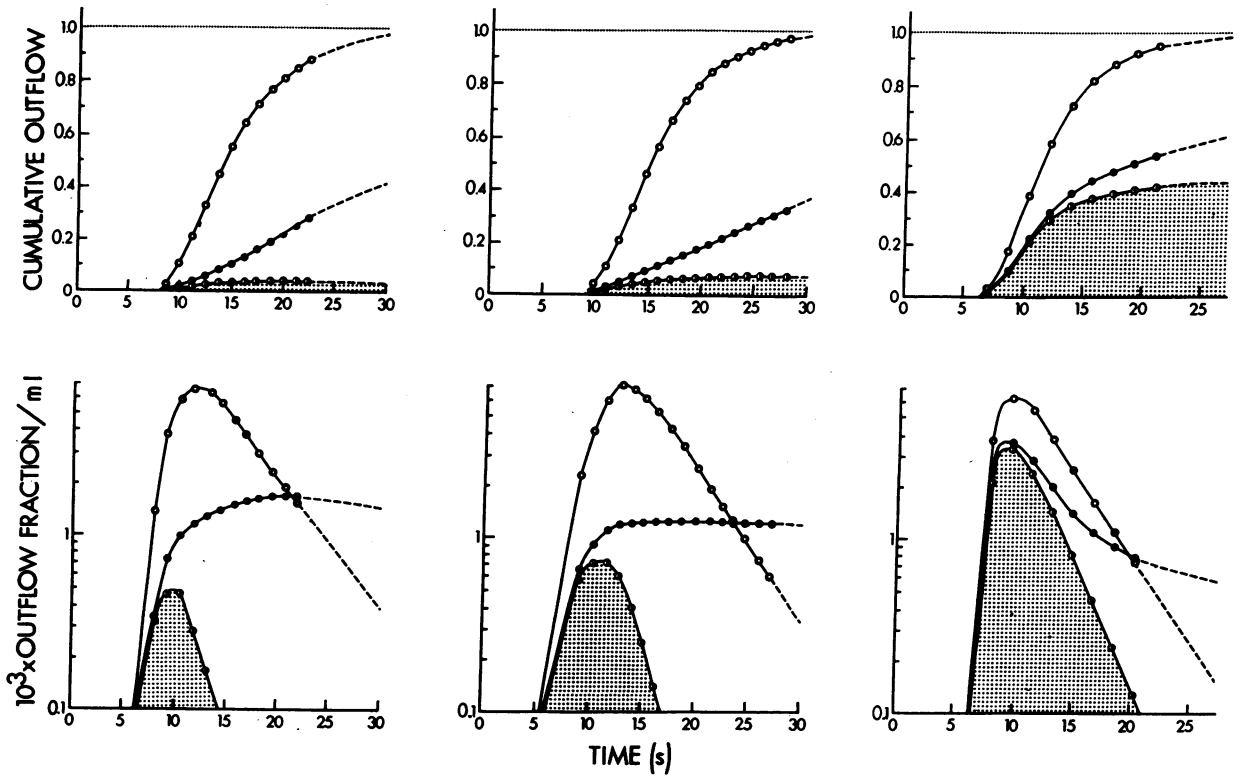

FIGURE 5 The computed best fit curves, for the experiments illustrated in Figs. 1 and 2. The left-hand and middle panels correspond, respectively, to the normal glucose and high glucose level experiments of Fig. 1; and the right-hand panel, to the high glucose level phlorizin infusion experiment of Fig. 2. In each panel the experimental sucrose curve is illustrated by open circles; and the computed tracer D-glucose curve, by closed circles. The throughput component of each tracer D-glucose curve is illustrated by half-filled circles and the area under it is shaded. The lower panels are semilogarithmic; and the upper panels, illustrating the cumulative outflows, are rectilinear. The values in the lower panels are plotted at mid-intervals; and those in the upper, at end-intervals.

determined by generating a computed glucose label curve from the sucrose curve, modifying the values until the sum of the squares of the differences between the experimental and computed tracer curves was minimized. The whole of the reliable experimental information (upslope, peak, and early downslope, to the time of recirculation of the sucrose label) was used to calculate these parameters. The aggregated values are displayed in Table II.

The model curves generated are composed of two components: throughput material, which sweeps past the cell surface without entering; and returning material, which has entered the cells and later returned to the plasma space. Fig. 5 illustrates the two components of the computed tracer D-glucose curves for the three cases: normal plasma glucose concentration, high plasma glucose concentration, and high plasma glucose concentration with concomitant intraportal infusion of phlorizin. The progressive increase in the proportion of material which comes through as throughput material is seen to account for the progressive change in the shape of the early parts of the labeled D-glucose curves. The cumulative outflows of the respective components of the curves are plotted in the upper panels of this diagram. The effectiveness of the curve-fitting process is illustrated in Fig. 6, for the two extremes illustrated in Fig. 5, the normal glucose level experiment and the phlorizin experiment. The coefficient of variation of the fit was 0.081 for the former, and 0.048 for the latter. For the whole series of D-glucose and phlorizin experiments the average coefficient of variation of the fit was 0.085.

The characteristic transport parameters. The kinetic coefficients computed have the dimensions ml s^{-1} ml^{-1}. For $k_1\theta/(1+\gamma)$ the dimensions are milliliters plasma transported per second per milliliter total space, vascular and extracellular, outside the cells; and for k_2 milliliters intracellular phase transported per second per milliliter intracellular space. The volume of intracellular phase is

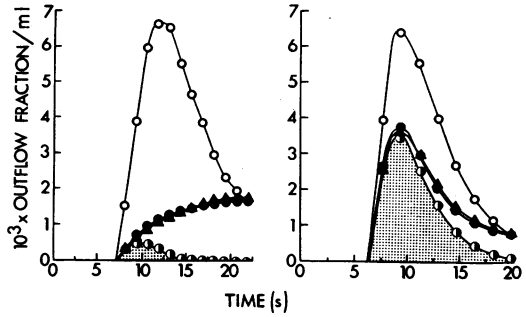

FIGURE 6 The experimental and best fit curves. The experimental tracer D-glucose curves are illustrated by filled triangles. The other symbols are the same as those in Fig. 5.

expressed in terms of an equivalent plasma volume. Each of the coefficients decreases with increase in the plasma glucose concentration (Fig. 7). Assume that the product of each kinetic coefficient and of the corresponding driving concentration (plasma or cellular) effectively repre-

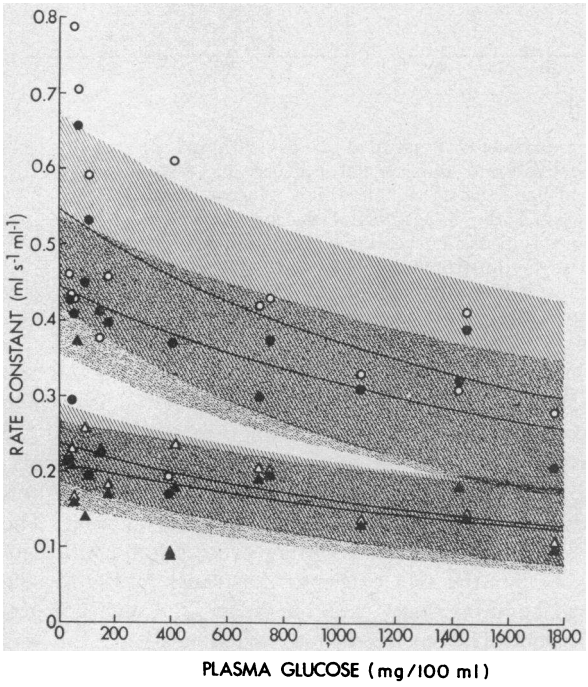

FIGURE 7 The relation between the kinetic coefficients derived from the experimental curves are represented in the following manner: $k_1\theta/(1+\gamma)$, filled circles; and k_2, filled triangles. A range of ±1.0 SE of the estimate around the best fit locus through these points is represented by dotted shading. Values for the same parameters, determined from the curves corrected for the delay and distortion introduced by the collecting system, are displayed as the corresponding open symbols; and the corresponding range about the best fit loci through these sets of points is represented by hatched shading.

sents an initial velocity of transport (mg s^{-1} ml^{-1}); and that the transport process is characterized by an asymptotic maximal velocity, V_{max}, and a plasma concentration corresponding to a half maximal velocity, a Michaelis-type constant or K_m. Then if a common relation is fitted to the data of Fig. 7, the coefficient predicted from this fitted relation will be, in each instance $V_{max}/([g]+K_m)$, where $[g]$ is the substrate concentration. For the coefficient $k_1\theta/[1+\gamma]$, $[g]$ will be the plasma glucose concentration; and for k_2, it should be the intracellular glucose concentration. We do not have access to the latter value but, in view of the apparent equivalence between the plasma and cellular glucose concentrations found in the tissue sampling experiments quoted above, it appears appropriate to set it equal to the plasma value. Optimal values for V_{max} and K_m are then obtained for each coefficient by minimizing the sum of squares of the differences between the observed coefficients and those predicted on the basis of the fitted relation (8). The characteristic parameters computed in this way are listed in Table III. We then corrected the dilution curves for the delay and distortion imposed by the catheter system (11), and derived from the new curves both a new set of kinetic coefficients and new values for the characteristic parameters. The latter differ little from the values derived from the original curves. For $k_1\theta/(1+\gamma)$ the V_{max} is 11.87 mg s^{-1} (milliliters total extracellular fluid)$^{-1}$; and, for k_2, 5.13 mg s^{-1} (milliliters intracellular fluid)$^{-1}$. In an equilibrative system, where $k_1 = k_2$, the ratio of the two coefficients, $k_1\theta/(1+\gamma)$ and k_2, is $\theta/(1+\gamma)$, the ratio of the intracellular space to the total accessible space outside the cells, sinusoidal plasma + extracellular space. For the glucose experiments the average value of the ratio of the coefficients derived from the curves corrected for catheter delay and distortion is 2.29; and the ratio of the computed V_{max} values, derived from the curves fitted to these coefficients, is 2.31. The concordance of these ratios is reassuring. In the above we have assumed that the partition coefficient for glucose in the intracellular water is unity, i.e., that

TABLE III

Parameters Providing the Best Fit to the Coefficients Derived from the Original and Corrected Curves

	V_{max} glucose		K_m glucose		K_i galactose	
Coefficient	Original	Corrected*	Original	Corrected*	Original	Corrected
	mg s^{-1} ml^{-1}		*mg/100 ml*		*mg/100 ml*	
$k_1\theta/(1+\gamma)$	11.13	11.87	2,500	2,180	594	—
k_2	5.51	5.13	2,600	2,160	3,110	—

* These values were derived from curves corrected for the delay and distortion imposed by the catheter collection system.

glucose is not excluded from any part of the aqueous phase. In this case the ratio then corresponds to the ratio between the cellular volume and the total space outside the cells, and the maximal rate of transport in either direction is calculated to be 5.13 mg s^{-1} (milliliters intracellular fluid)$^{-1}$. The two K_m values calculated from the corrected curves, that for influx and that for efflux, are virtually equal, and average 2,170 mg/100 ml. This equality is also expected in an equilibrative transport system (12), and it is reassuring to find that the two values derived from these data are equal.

The effect of galactose infusion. The shape of the tracer D-glucose curve after galactose loading to plasma levels of approximately 400 mg/100 ml corresponds to that expected for correspondingly much higher levels of plasma glucose. In the animals fasted overnight but not given galactose, the plasma galactose levels were very low, and ranged from 0 to 6 mg/100 ml. In the following, the galactose levels in these experiments will therefore be assumed, for the sake of simplicity, to be equivalent to zero. On the contrary the plasma glucose levels in the galactose-loaded animals averaged 128 mg/100 ml and corresponded to those found in fasted animals not loaded with glucose. To interpret the changes in the shape of the tracer D-glucose curve and the changes in the calculated coefficients $k_1\theta/(1+\gamma)$ and k_2, we then assumed that the galactose-loading effect was mediated by competitive inhibition at the transport site. Hence, if we proceed as above and fit a common relation to the data, the apparent K_m of the fit will be $K_m(1+[i]/K_i)$ where $[i]$ is the concentration of galactose, K_i is the Michaelis-type constant characterizing the effect of the inhibitor, galactose, upon the transport process for tracer glucose, and K_m is the value which we previously derived from the glucose data. Each predicted coefficient may therefore be set equal to $V_{max}/(K_m(1+[i]/K_i)+[\bar{g}])$, where the value taken for $[\bar{g}]$ is the average glucose level for the galactose-loaded experiments, and the values for V_{max} are those derived above from the glucose experiments. The fitted value for the K_i derived for $k_1\theta/(1+\gamma)$ is 594 mg/100 ml; and that for k_2, 3,110 mg/100 ml. The latter corresponds to a value far above the range of the experiments. In the galactose-loaded experiments the transit times were unexpectedly short and the number of points on the dilution curves were consequently relatively small. In this set of circumstances the procedure for correcting the curves for the delay and distortion produced by the collecting system becomes inaccurate (7); and so the K_i value was not computed for the corrected curves.

The effect of phlorizin. The steady intraportal infusion of phlorizin has reduced both the entry and efflux coefficients for tracer D-glucose more or less symmetrically. Both coefficients are, in each instance, substantially below the levels expected at the corresponding D-glucose levels.

The L-glucose and β-methyl D-glucoside experiments. The L-isomer, the mirror image of D-glucose, is not only not utilized; it also enters the liver cells very slowly. The average proportion of the L-glucose emerging as throughput material is 0.923, in these experiments. The proportion taken up is small. Similarly, the replacement

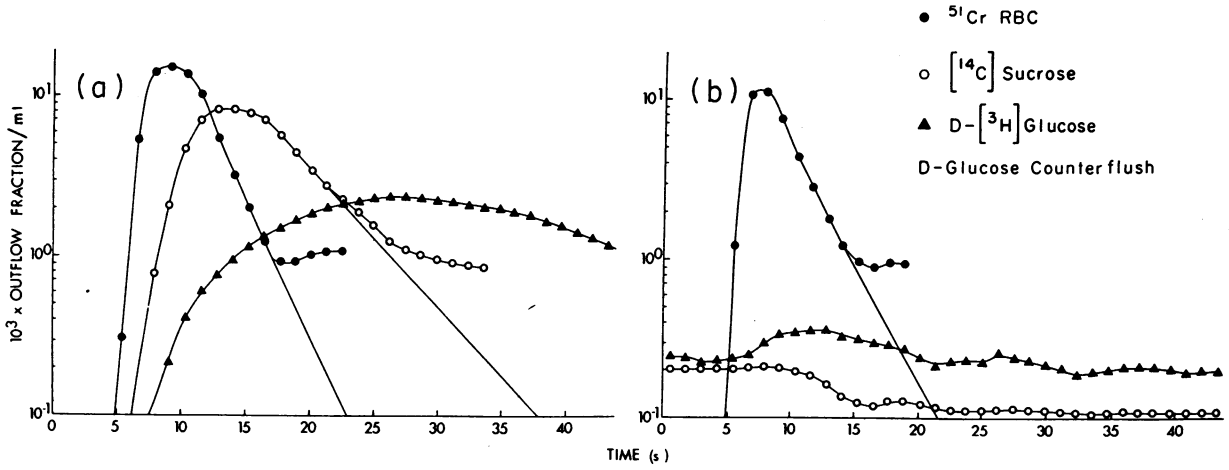

FIGURE 8 The countertransport of labeled D-glucose. (*a*) This panel illustrates the initial run. The plasma glucose concentration was 87 mg/100 ml. (*b*) This panel shows the effect of a sudden infusion of hypertonic glucose upon the plasma activities of the labeled sucrose and D-glucose, 2 min after the first injection. A marker bolus of red cells has been injected at the beginning of this infusion.

of the equatorial β-hydroxyl group of the Cl form of the glycopyranoside by a methoxy group results in a loss of affinity of the molecule for the glucose transport system. The average proportion emerging as throughput material in the β-methyl D-glucoside experiments is 0.952. An even smaller proportion has entered the cells.

The countertransport of labeled glucose. One of the usual phenomena displayed by a membrane carrier transport system is the countertransport of labeled substrate (13). We therefore designed an in vivo experiment to search for this phenomenon. An ordinary run was carried out first, in which labeled red cells, labeled sucrose, and labeled D-glucose were injected (experiment 1 in the Tables, and Fig. 8*a*). After 2 min a countertransport experiment was carried out in the following way: a bolus of labeled red cells was flushed from a cuvette into the portal vein and followed for the next 10 s by 50 ml of 50% D-glucose. The results are displayed in Fig. 8*b*. The usual red cell dilution curve was derived from the increment in labeled red cell activity. The labeled D-glucose and sucrose activities are displayed as continuations of the curves of the Fig. 8*a*. Two phenomena are evident. First, the labeled sucrose activity abruptly decreases to a lower level, at the time the throughput hypertonic glucose would be expected to emerge. A baseline dilution of the activity has occurred (14), due to the net flux of water across the cell surfaces, induced by the hypertonic glucose. Second, the labeled glucose curve, instead of following the labeled sucrose curve and decreasing, increases and the two curves initially diverge. The increase then ceases and the two curves change in a more or less parallel fashion. The contrary change of the two curves, after arrival of the hypertonic glucose, and the apparent increment in the area between them provides striking evidence for the induction of the countertransport of labeled D-glucose, in this experiment. The observations were found to be reproducible in the sense that similar phenomena were induced in two other animals.

DISCUSSION

The extracellular reference substance. In these multiple indicator dilution experiments the reference substance should be a material which behaves in every way identical to the substance being studied, except that it does not participate in the process under examination (15). We selected labeled sucrose as an appropriate extracellular reference, a substance which is not transported. In the isolated perfused liver, it is completely excluded from the liver cells (6). In the intact animal, the apparent volume of distribution of labeled sucrose in the liver increases slowly, as a result of the hydrolysis and reabsorption (as monosaccharide) of the small amounts secreted in bile (16). Over short times this process is not quantitatively significant. Inulin was considered not to be a suitable reference, because it is excluded from a major part of the extracellular space, by virtue of a partition phenomenon dependent upon its molecular size (10, 17). Because of this lack of suitability, data incorporating inulin as an extracellular reference (such as those of Williams et al. [6]) must be considered to be an inappropriate experimental base for the computation of transport parameters. One might expect a small but similar partition phenomenon to produce a minor effect on the distribution space for disaccharides in the extracellular space of the liver, and, on this basis, a nontransported monosaccharide would be a more ideal reference. We were unable to find this kind of compound; and, in view of the observed close relation between the labeled β-methyl D-glucoside and sucrose curves, consider that there is no evidence for such a differential partition phenomenon, at this lower molecular size level.

The form of the outflow curves. This study characterized the components of the outflow profile for a substance entering and leaving the liver cells by an equilibrative transport system. Under this particular set of circumstances the two characteristic outflow components, throughput and returning material, overlap to a very considerable extent. The basis for the resolution of the components of the outflow curves lies in the distributed modeling which we previously developed and which we have utilized here (7). In the case we previously analyzed, that of a highly concentrative transport system (for ^{86}Rb), we demonstrated that the early part of the outflow curve was essentially almost completely throughput material, with proportionately very little returning material and we were able to match fairly precisely the form of the throughput material. The ability to predict the relative form of the throughput material in this concentrative system gave us confidence that, in the situation analyzed here, where throughput and returning material are inextricably intermixed, the throughput component would be relatively accurately predicted; and the relatively good fit to the whole curve found indicates that a fair degree of confidence may also be placed in the fit to the second component. The modeling furthermore accounts for the variety of shapes of dilution curves encountered with elevation of the plasma glucose levels, introduction of galactose or phlorizin, and changes in the molecular architecture of the tracer glucose probe.

Bravo and Yudilevich have carried out similar dilution studies of tracer glucose uptake by the liver. At ordinary plasma levels, curves similar in form to those presented here were found (18). These authors did not

carry out an analysis detailed enough to yield estimates of the transport coefficients.

The transport paramcters. The transport of D-glucose shows the characteristics expected of an equilibrative carrier-mediated transport system: saturation kinetics, competitive inhibition, isotope countertransport, and stereospecificity. The V_{max} calculated for the liver cells, 5.13 mg s^{-1} ml^{-1}, is exceedingly rapid. It is approximately three times the transport maximum for human erythrocytes (12) and is many times larger than the maximum observed rate of entry of glucose into dog red cells. The K_m for the glucose entry and exit processes, 2,170 mg/100 ml, is also large. Saturation of the initial velocity of tracer uptake was demonstrated only by raising the glucose concentrations to exceedingly high levels. Over the physiological range the fluxes remained almost proportional to the plasma levels.

Galactose exhibited a peculiar competitive effect. For the tracer D-glucose entry process its K_i was 594 mg/100 ml and elevation of the plasma galactose was fairly effective; but for the exit process, its K_i was a value much higher than the levels used experimentally (that is, there

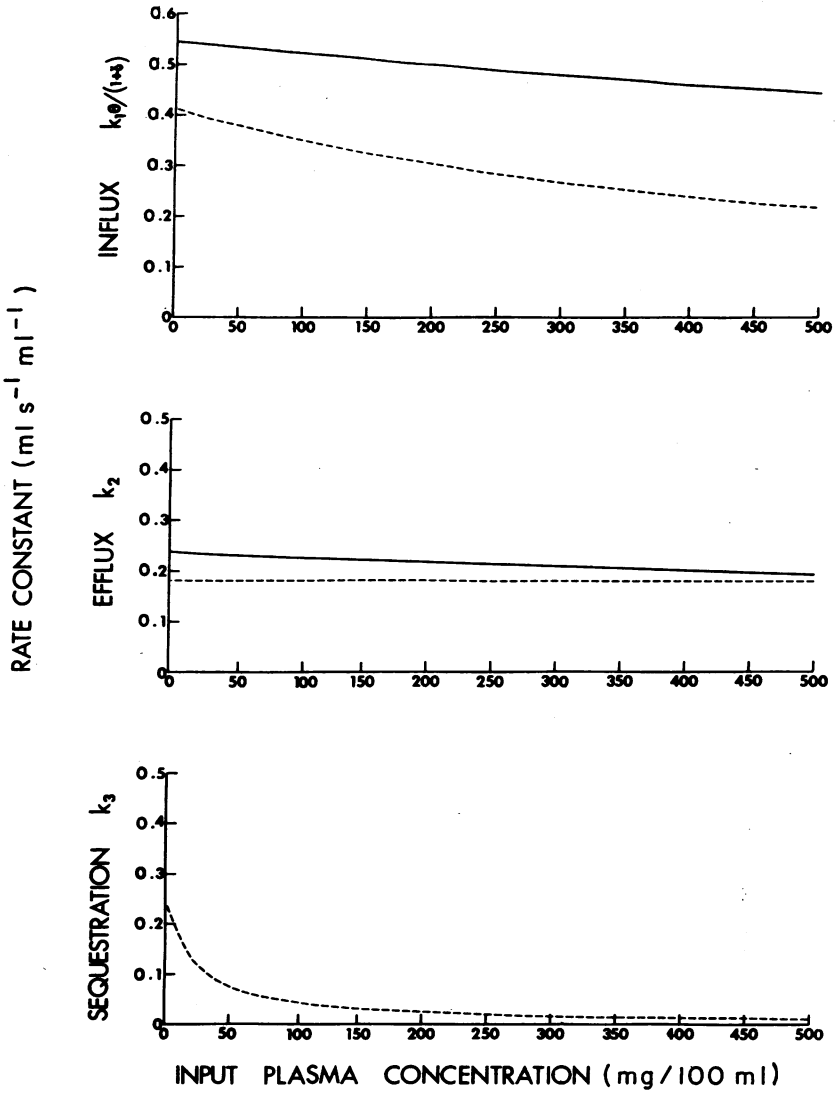

FIGURE 9 Comparison of the manner in which the process rate constants for glucose and galactose change with the corresponding input plasma sugar concentration. The continuous lines reproduce the fitted relations derived from the present tracer D-glucose data, corrected for catheter effects; and the dashed lines, those derived from the corrected tracer D-galactose experiments of reference (8).

TABLE IV

The Michaelis-type K_m and K_i Transport Parameters

Substrate whose concentration was varied	$k_1\theta/(1+\gamma)$ parameters		k_2 parameters	
	Glucose*	Galactose*	Glucose*	Galactose*
	mg/100 ml		*mg/100 ml*	
Glucose	2,180	1,500	2,160	1,350
Galactose	594	514	Very large	Very large

* The kinetic coefficients, from which the K_m and K_i values were derived, come from outflow curves for this tracer substance.

was relatively little evidence of inhibition). Scriver and Wilson (19) have proposed that if the K_m of a transport substrate at its own site and its K_i at a second site at which it acts as a competitive inhibitor are the same, the two sites may be identical; and this hypothesis is strengthened if the values are also identical when the test is done in reverse. It is appropriate to examine both our present data and that arising from our previous galactose study (8) from this point of view (see Table IV). For the tracer D-galactose entry process the K_m for galactose was 514 mg/100 ml, so the K_i and K_m for this substance are virtually identical. The K_i for glucose, inhibiting tracer galactose entry, was 1,500 mg/100 ml. This value was based on a small number of studies, and it therefore appears that this value and the K_m for glucose, 2,170 mg/100 ml, may not be remarkably different. Similarly for the exit process both the K_m for galactose and the K_i for galactose inhibition are very high values (far above the experimental concentration range); and for glucose the K_i for tracer galactose inhibition was 1,350 mg/100 ml, a value lower but not substantially different from the K_m for glucose Although the K_m and K_i values are not in every instance very close it does appear reasonable to construe that, for both entry and exit processes, glucose and galactose share a common process. In view of the observation of linked glucose-galactose malabsorption in some families (20), the basis for this shared process may well be a common mammalian gene.

One other aspect of the transport parameters bears comment. We previously alluded to the expectation that when a transport system is equilibrative, the K_m value for entrance and exit would be the same; and the expectation that, when the K_m for exit is much larger than that for entry, the process would be found to be concentrative. The values found for galactose transport appeared to fit the latter case yet no confirmatory evidence for the concentrative nature of the process was available from tissue sampling experiments, at the time of the original study. It is therefore reassuring to find that, during galactose infusion, the concentration of free galactose in the cellular water of liver biopsies becomes significantly higher than that in the input plasma water, when metabolic galactose sequestration is impeded by concomitant ethanol infusion (21).

The characteristic transport parameters for glucose and galactose, by themselves, do not provide the reader with an easy grasp of the comparative ways in which the kinetic coefficients of these two substrates vary with input plasma concentrations. To provide this comparison we have plotted Fig. 9. The kinetic coefficients $k_1\theta/(1+\gamma)$ and k_2 are somewhat larger for glucose than they are for galactose, but are not remarkably different in magnitude. The principle difference between the handling of the two sugars is in the sequestration constant k_3. This rate constant is relatively large in magnitude for galactose, especially at lower levels of sugar concentration, but has not been found to be high enough to be reliably measured by our experimental approach, in the case of glucose.

The effect of phlorizin. In the present experiments the competitive effect of phlorizin would have been expected to be related to its presence and interaction at the transport site. In preliminary experiments we had found that the phlorizin, given as a single intravenous dose 30 min before an experimental run, produced little measurable change in the hepatic transport of D-glucose. We therefore used instead a steady intraportal infusion of phlorizin and found the effect reported above, a symmetrical reduction of both influx and efflux coefficients for tracer D-glucose. The lack of effect of the single dose, a half hour after administration, was undoubtedly due to its removal from the circulation, in large part by its concentrative accumulation in the kidney (22).

The amounts of phlorizin necessary to demonstrate inhibition of the hepatic transport system were comparatively high. Silverman, Aganon, and Chinard, for instance, found complete inhibition of the D-glucose transport system at the luminal surface of the renal tubule, at rates of infusion less than 0.001 times the rate used here. They also observed that tracer D-glucose entered the renal tubular cells from the vascular or antiluminal surface; and that the sensitivity of this entry process was comparatively low. Entry was inhibited by phlorizin only when rates of infusion were raised to values similar to those which we utilized in our present series of experiments (23). Similarly, in their tissue sampling experiments, Williams et al. (6) found that comparatively high levels (10^{-2} M) of phlorizin were necessary to produce substantial inhibition of the hepatic transport of D-glucose.

The production of glucose by the liver. In the normal animal, when the plasma glucose is less than 90 mg/100 ml and net hepatic glucose production begins to occur (2, 3), the modeling which we have used in our analysis is incomplete. At lower plasma levels glucose is being generated, presumably in each cell along the sinusoidal length, and is being added to the intracellular pool. If portal vein and hepatic arterial flows can be considered to be mixed at the origin of the sinusoids, this addition will result in a gradient in concentration, an increase in both the intracellular and sinusoidal concentrations, from the portal triad to the central vein areas of each lobule. Our modeling of glucose exchange has not taken this additional process into account. We have not incorporated into the modeling the effect of this added flux, the addition of unlabeled glucose to the intracellular space (24). Its addition would complete the modeling so that it would then correspond more accurately to the processes underlying glucose homeostasis. Nevertheless, despite this defect at low plasma glucose levels, our analysis does appear to provide the first accurate in vivo estimates of the parameters characterizing the hepatic glucose transport system.

The design of the liver. The liver lobules are characterized by sinusoids with adjacent entrances and adjacent exits, and concurrent flow. Where substances are being consumed a gradient in concentration occurs (8), with lower concentrations in the center of the lobules. In the case of oxygen, this will be expected to create zones of lowered P_{O_2} in the centers of the lobules. At first inspection one would consider the liver to be a poorly designed system, from this point of view. However, if we examine it from the point of view of a process like glucose production, alluded to above, a major advantage appears. A large step-up in concentration, from portal vein to hepatic vein, can be achieved without a major step-up in concentration at any particular cell. The advantages are analogous to those of a countercurrent multiplier system where, by virtue of the length of the system, the single effect is greatly increased. Removal processes can be viewed similarly. A large portal vein-hepatic vein difference can be created, without a large demand on each cell. Thus we can conclude that, from the point of view of its function as essentially a chemical factory, the liver has a superb architectural design. This enables the work demanded of each hepatic cell to achieve an overall effect, to be minimized.

ACKNOWLEDGMENTS

We wish to express our appreciation to Mrs. Heather Kennedy, for her expert technical assistance; and to Miss Margaret Mulherin, for typing this manuscript.

We are indebted to the Medical Research Council of Canada and the Quebec Heart Foundation for their generous financial support; and to the Elliott-Cerini Foundation for facilitating the early stages of the analysis of these data.

REFERENCES

1. Soskin, S., H. E. Essex, J. F. Herrick, and F. C. Mann. 1938. The mechanism of the regulation of the blood sugar by the liver. *Am. J. Physiol.* **124**: 558.
2. Combes, B., R. H. Adams, W. Strickland, and L. L. Madison. 1961. The physiological significance of the secretion of endogenous insulin into the portal circulation. IV. Hepatic uptake of glucose during glucose infusion in non-diabetic dogs. *J. Clin. Invest.* **40**: 1706.
3. Madison, L. L. 1969. Role of insulin in the hepatic handling of glucose. *Arch. Intern. Med.* **123**: 284.
4. Cahill, G. F., Jr., J. Ashmore, A. S. Earle, and S. Zottu. 1958. Glucose penetration into liver. *Am. J. Physiol.* **192**: 491.
5. Goresky, C. A. 1967. The distribution of substances in a flow-limited organ, the liver. *In* Compartments, Pools, and Spaces in Medical Physiology. P. E. Bergner and C. C. Lushbaugh, editors. U. S. Atomic Energy Commission, Division of Technical Information, Oak Ridge. 423.
6. Williams, T. F., J. H. Exton, C. R. Park, and D. M. Regen. 1968. Stereospecific transport of glucose in the perfused rat liver. *Am. J. Physiol.* **215**: 1200.
7. Goresky, C. A., G. G. Bach, and B. E. Nadeau. 1973. On the uptake of materials by the intact liver. The concentrative transport of rubidium-86. *J. Clin. Invest.* **52**: 975.
8. Goresky, C. A., G. G. Bach, and B. E. Nadeau. 1973. On the uptake of materials by the intact liver. The transport and net removal of galactose. *J. Clin. Invest.* **52**: 991.
9. Crane, R. K. 1962. Hexokinases and pentokinases. *In* The Enzymes. P. D. Boyer, H. Lardy, and K. Myrback, editors. Academic Press, Inc., New York. 2nd edition. 47.
10. Goresky, C. A. 1963. A linear method for determining liver sinusoidal and extravascular volumes. *Am. J. Physiol.* **204**: 626.
11. Goresky, C. A., and M. Silverman. 1964. Effect of correction of catheter distortion on calculated liver sinusoidal volumes. *Am. J. Physiol.* **207**: 883.
12. Silverman, M., and C. A. Goresky. 1965. A unified kinetic hypothesis of carrier mediated transport: its applications. *Biophys. J.* **5**: 487.
13. Wilbrandt, W., and T. Rosenberg. 1961. The concept of carrier transport and its corollaries in pharmacology. *Pharmacol. Rev.* **13**: 109.
14. Effros, R. M. 1972. Impairment of red cells transit through the canine lungs following injections of hypertonic fluids. *Circ. Res.* **31**: 590.
15. Chinard, F. P., G. J. Vosburgh, and T. Enns. 1955. Transcapillary exchange of water and other substances in certain organs of the dog. *Am. J. Physiol.* **183**: 221.
16. Forker, E. L. 1970. Hepatocellular uptake of inulin, sucrose, and mannitol in rats. *Am. J. Physiol.* **219**: 1568.
17. Brauer, R. W. 1963. Liver circulation and function. *Physiol. Rev.* **43**: 115.
18. Bravo, I. R., and D. L. Yudilevich. 1971. Liver dis-

tribution and uptake of molecules studied by rapid indicator-dilution technique. *Am. J. Physiol.* **221**: 1449.

19. Scriver, C. R., and O. H. Wilson. 1964. Possible locations for a common gene product in membrane transport of amino-acids and glycine. *Nature* (*Lond.*). **202**: 92.
20. Elsas, L. J., R. W. Hillman, J. H. Patterson, and L. E. Rosenberg. 1970. Renal and intestinal hexose transport in familial glucose-galactose malabsorption. *J. Clin. Invest.* **49**: 576.
21. Keiding, S., N. Tygstrup, F. Vallø-Hansen, and K. Tønneson. 1973. Modification of galactose elimination kinetics by ethanol in the perfused pig liver. *In* Regulation of Hepatic Metabolism (Alfred Benzon Symposium VI). F. Lundquist and N. Tygstrup, editors. A/S Munksgaard, Copenhagen. In press.
22. Diederich, D. F. 1966. Glucose transport carrier in dog kidney: its concentration and turnover number. *Am. J. Physiol.* **211**: 581.
23. Silverman, M., M. A. Aganon, and F. P. Chinard. 1970. D-Glucose interactions with renal tubule cell surfaces. *Am. J. Physiol.* **218**: 735.
24. Hetenyi, G., Jr., K. H. Norwich, D. R. Studney, and J. D. Hall. 1969. The exchange of glucose across the liver cell membrane. *Can. J. Physiol. Pharmacol.* **47**: 361.